3: Engineered Wire Elements

Microwave absorber based on engineered wire element is the simplest absorber in terms of tuning of resonant frequency, reduced reflection in cross-polarization and ease of fabrication using low-cost screen printing technique. The resonant frequency of Wire-Based Absorber (WBA) inversely to the wire element length and permittivity of the material [Pang *et al.*, 2013]. The cross-polarization reflection of WBA is almost nil due to the dipole nature of the wire element. The additional resonance modes can be introduced using WBA by changing the wire element length. Multiband, bandwidth-enhanced and wideband absorbers are designed and analyzed using engineered planar WBA.

3.1 WBA MULTIBAND

Multiband absorbers mostly consist of complex geometry viz. arrow resonator [Li *et al.*, 2011], [Bian *et al.*, 2013], [Zhu *et al.*, 2010]. They are difficult to design and analyze in terms of tuning of resonating frequency because of the coupling effect between elements. Moreover, the fabrication of these complex geometries is as well as time-consuming and costly.

Considering this, multiband (single/dual/triple band) absorbers based on wire elements are designed, fabricated and measured. The reported wire-based absorbers are polarization-dependent due to single wire elements [Pang *et al.*, 2013]. In contrast to this, the proposed absorbers consist of one/two/three metallic wire elements (placed vertically and horizontally for polarization independence) for single/dual/triple band absorption. These metallic wires are printed on lossy FR4 sheet backed with a metallic plate.

The absorption mechanism for the multiband wire-based absorbers can be explained in terms of the RLC circuit. The wire elements (printed on a dielectric substrate) and the bottom metal plate forms a cavity. The circulating currents in the wire elements and the lower metal plate induces L, whereas the sandwiched dielectric material between the wire elements and the lower metal plate works as C [Pang *et al.*, 2013]. The losses are attributed to the metallic wires and the lossy dielectric substrate.

The resonant frequency is tuned by changing the metallic wire length. The proposed absorbers are polarization insensitive due to the four-fold rotational symmetry of the designed absorbers.

3.1.1 Multiband Absorber: Design

The initial design regarding wire element length is based on commercial available FR4 sheet, the measurement set up and ease of fabrication using a low-cost screen printing facility. The FR4 laminate is selected owing to low cost, no-toxicity, ease of availability, copper coating and prevalent use for microwave applications. The side view of the unit cell of the proposed single/multi-band absorbers is shown in Figure 3-1(a). The absorbers consist of metallic wires on metal grounded FR4 sheet. The permittivity and loss tangent of the FR4 sheet are 4.2 and 0.02, respectively. The front view of proposed single, dual, triple band absorbers are shown in Figure 3-1 (b), (c), (d). The single/dual/triple band absorber consists of one/two/three metallic wire respectively. The metallic wires are made up of copper with conductivity 5.8×10^7S/m. The design parameters for maximum absorbance are p=20, d=1, t_{co}=0.035, w=0.8, l_1=7.5, l_2=7, l_3=6.5, l_4=5.5, l_5=6.6, l_6=8, g_1= g_5=8, g_2= g_3=2, g_4=5mm.

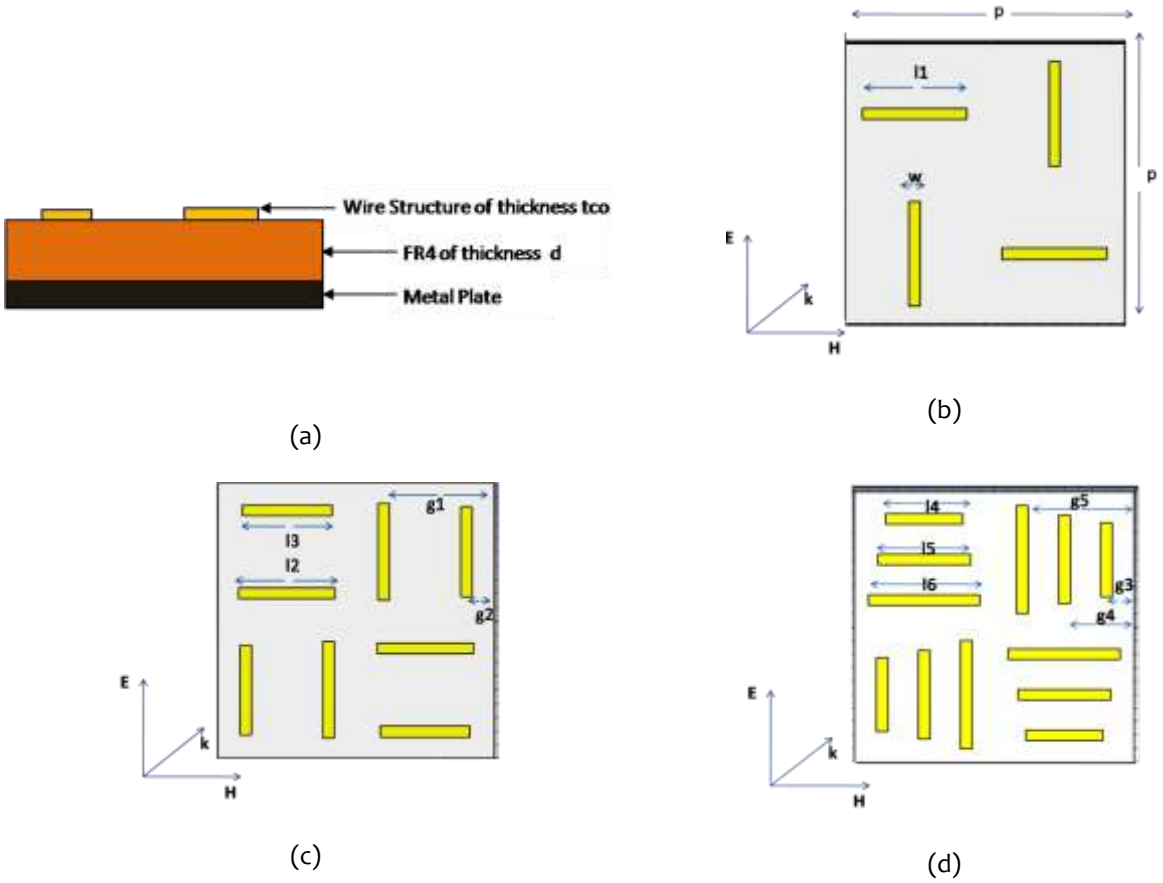

Figure 3-1 :(a) Side view and Front view of a unit cell of the (b) single (c) dual (d) triple-band absorbers

Based on design parameters, the fabricated single/dual/triple band absorbers are shown in Figure 3- **2**, using a screen printing technique. The dimensions of fabricated absorbers are 124mm × 124mm × 0.5mm approximately.

(a) (b) (c)

Figure 3- 2: Fabricated (a) triple, (b) dual and (c) single-band absorber

3.1.2 Simulation and Measurement Results

The absorbance of proposed absorbers is given by $A(\omega) = 1 - |S_{11}|^2$. The full EM wave simulation of the proposed absorbers was carried out in CST Microwave Studio to obtain S parameters for wave vector, electric field and magnetic field direction are shown in Figure 3-1. The single/multi-band absorbers are investigated for different polarization angle. The designed absorbers are polarization insensitive due to four-fold rotational symmetry.

The S-parameters of absorbers are measured using vector network analyzer and a pair of the horn antenna. The measured absorbance peak for single-band absorber is 10.2 GHz, for dual-band 10.8 & 11.5 GHz for triple-band absorber 9.4, 11.2 & 13.2 GHz. For wire-based metamaterial absorber, the resonant frequency varies inversely to wire length for given permittivity. The higher resonant peaks are due to lower wire length, and lower frequency peaks are due to higher wire length. From experimental results Figure 3-3 (a), (b) and (c), it is observed that for single-band absorber, there is good agreement between experimental and simulation results. Subsequently, for the dual-band and triple-band absorbers, there is a slight deviation in experimental and simulation results. This may be attributed to a small sample size of fabricated absorbers and fabrication error.

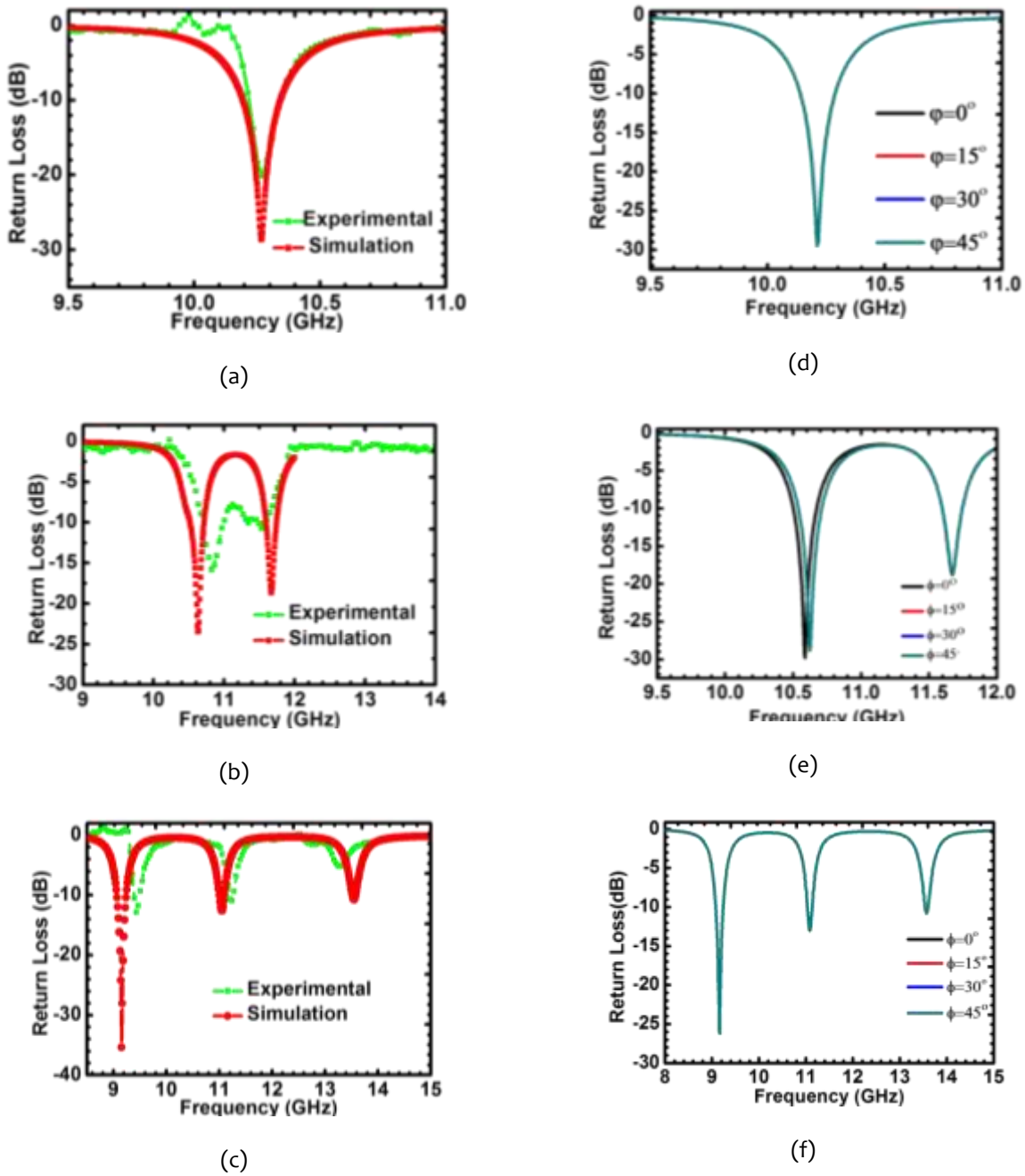

Figure 3-3: Return loss (measured & simulated) and variation of polarization angle (simulated) (a, d) for single, (b, e) dual, and (c, f) triple-band absorber

The designed absorbers are numerically investigated for the polarization angle 0^{o} to 45^{o}. The response of single, dual and triple-band absorbers are presented in Figure 3-3(d), (e) and (f).

`
The proposed absorbers are insensitive to polarization angle due to four-fold rotational symmetry.

As a conclusion, the design methodology for multiband polarization-insensitive absorbers using engineered wire element is demonstrated. The resonant frequency can be adjusted using the wire length.

3.2 WBA: BANDWIDTH-ENHANCED

The engineered planar absorber can be modelled as RLC circuit. The equivalent circuit model for the WBMA can be modelled as an RLC circuit, where R term accounts form the finite conductivity of metallic wire and lossy substrate [Pang et al., 2013]. The resonant frequency and corresponding quality factor associated with the RLC circuit are given by $f = \frac{1}{2\pi\sqrt{LC}}$ and $Q = (\frac{1}{R})\sqrt{\frac{L}{C}}$ respectively [Gu *et al.*, 2010]. The resonant frequency can be tuned by changing the L and C parameters, i.e. by changing the wire dimensions, scaling of the unit cell, substrate parameters and thickness. The metamaterial absorbers show narrow band (high Q-value) absorption, which can be broadened by inserting the resistive losses in the structure [Pang *et al.*, 2011], [Cheng *et al.*, 2013].

In spite of using resistive components, the bandwidth can be improved by inducing multiple resonance modes. The tuning of design parameters selectively overlaps these modes, which result in bandwidth enhancement. The resonance frequency of wire-based absorber varies inversely with wire element length and permittivity of the substrate [Pang *et al.*, 2013]. Using multiple wires of different length results in bandwidth enhancement by overlapping of multiple absorption frequencies. Taking advantage of this fact, the bandwidth-enhanced wire-based absorber is designed, analyzed, fabricated and characterized.

The design comprised of multiple wires printed on metal grounded lossy dielectric substrate. The proposed structure is fabricated using the screen printing technique. The improved bandwidth is attributed to the overlap of the absorption peaks of individual wires. Results show that bandwidth of proposed absorber corresponding to 10dB return loss is 0.5 GHz. The simulated bandwidth of the proposed absorber is independent of the variation in incidence angle from 0^o to 30^o.

3.2.1 Design Parameters

The side view of the unit cell of the Multiple Wire-Based Microwave Absorber (MWBMA) is shown in Figure 3- 4(a). The absorber consists of a metal plate, FR4 sheet and a metallic structure, as shown in Figure 3- 4(b). The relative permittivity and loss tangent of the FR4 sheet is 4.3 and 0.025, respectively. The wire element consists of copper with electric conductivity 5.7×10^7 *S/m*. The lengths of copper wires are selected to have closely spaced absorption peaks to achieve large bandwidth. The structure dimensions are tuned for maximum absorption, which is obtained at 9.7 GHz with the design parameters: p=20, d=1, t_{co}=0.035, w=0.8, l_1=7.6, l_2=7.8, l_3=8.0, l_4=8.15, l_5=7.7, g_1=5, g=10mm.

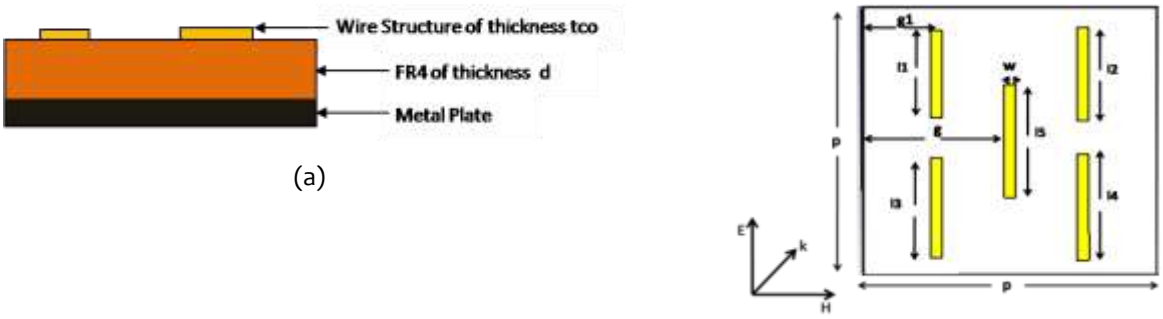

Figure 3- 4: (a) Side View (b) Front view of the unit cell of the proposed absorber

The proposed absorber is fabricated using the screen printing technique. The fabricated absorber is shown in Figure 3-5(a). The dimensions of fabricated absorbers are 134 mm x 132 mm × 1mm approximately. The performance of absorber is measured using vector network analyzer and a pair of the horn antenna. The absorber is characterized for normal incidence. Due to sample size limitation, the measurement for different incident angles cannot be performed.

3.2.2 Fabrication and Measurements

The proposed structure is evaluated for incidence by z-propagating electromagnetic (EM) wave with magnetic and electric fields x and y-axis respectively, as shown in Figure 3- 4 (b). Full-wave EM simulation of the proposed absorber is carried out using CST Microwave Studio, and S-parameters are obtained. The electromagnetic wave absorption of a metal-backed structure is given by $A(\omega) = 1-R(\omega)-T(\omega)$. The absorbance can be calculated from S-parameters using $A=1-|S_{11}|^2-|S_{21}|^2$. For metal back absorber $|S_{21}|=0$, the absorbance is given by $A=1-|S_{11}|^2$.

The measured and simulated return loss of the absorber for normal incidence is depicted in Figure 3-5(b). It is observed that there is good agreement between experimental and simulated results. The proposed absorber shows a bandwidth of 0.5 GHz for 10 dB return loss. The measurement results show two return loss peaks of 14.2 dB and 24.1 dB at frequencies 9.3 and 9.6 GHz, respectively.

Consequently, the bandwidth corresponding to 10 dB return loss is nearly constant for the angle of incidence 0^0 to 30^0 and decreases with further increase in incidence angle as the second peak vanishes. The variation of bandwidth with a large angle of incidence is due to weak magnetic coupling between the top layer and bottom layer. The magnetic field is not effective to drive magnetic resonance in the absorber. For a large angle of incidence, the absorber is driven by electric field only. Hence there is impedance mismatch due to which there is a significant decrease in the bandwidth of absorber, the vanishing of the second resonant peak at large angle of incident is attributed to the non-uniform excitation of the absorber elements.

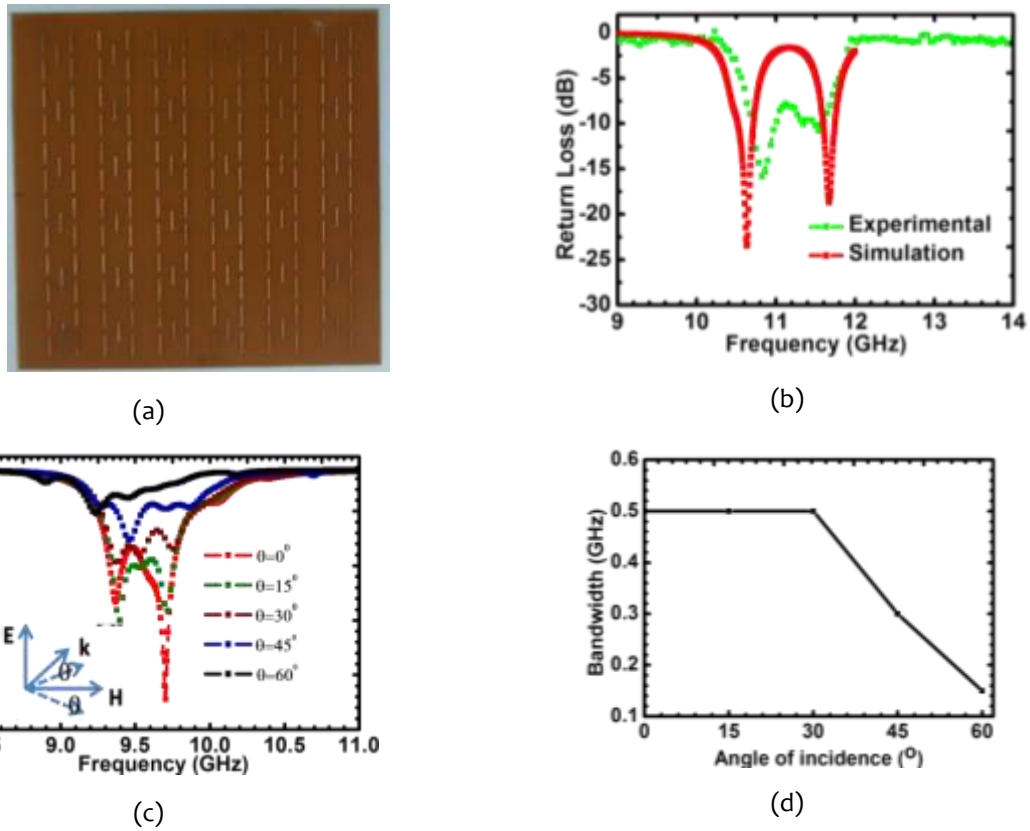

Figure 3-5: (a) Fabricated Absorber (b) Experimental and simulated Return loss for normal incidence, (c) Simulated Return loss for 0-60o incidence, (d) Bandwidth variation with incidence angle

As a conclusion, a multiple wire-based metamaterial absorber is designed and fabricated. The bandwidth of absorber is enhanced due to the overlap of the individual wire response. Nevertheless, due to lack of the fourfold symmetry, this design is polarization sensitive.

3.3 WBA WITH DIELECTRIC CAP

The limitations associated with metamaterials absorbers are narrow absorption bandwidth and high reflection in cross-polarization because of resonating structure and the absence of resistive components respectively. The physical insight of metamaterial absorber lies in the equivalent RLC circuit model [Pang *et al.*, 2013]. The equivalent impedance of metamaterial absorber is expressed as:-

$$\frac{1}{Z_i} = \frac{1}{Z_{FSS}} + \frac{1}{Z_d} \qquad (1)$$

$$Z_{FSS} = R + j\omega L + \frac{1}{j\omega C} \qquad (2)$$

$$Z_d = Z_0\sqrt{\frac{\mu}{\varepsilon}}\tanh\left(j\frac{2\pi f d}{c}\sqrt{\varepsilon\mu}\right) \qquad (3)$$

where Z_{FSS} and Z_d are the impedances due to the equivalent RLC model and material, respectively. Further, Z_0, f, d, c, ε and μ is the free space impedance, frequency, thickness, speed of light, permittivity and permeability of the material absorber respectively. The finite conductivity of metal and loss tangent of the substrate introduces R, anti-parallel current arises L and coupling between the nearby unit cell induce C. The resonance occurs due to resonating circuit [Pang *et al.*, 2013] and contribution due to Z_d is missing owing to low loss tangent of dielectric materials for example FR4.

Wire-Based Metamaterial Absorber (WBMA) is capped with dielectric absorber is investigated. The WBMA shows a single resonance peak due to $Z_{FSS,}$ whereas Z_d peak appears because of the dielectric absorber. The tuning of design parameters results in merging of peaks and gives a bandwidth of more than 6 GHz for 10 dB return loss. The unit cell of the designed absorber consists of copper wires, placed on the metal back FR4 sheet and dielectric absorber are located on the top of wire elements. The simulated return loss shows two resonant modes, one due to the dielectric absorber and other due to wire-based metamaterial absorber. The electric field and power loss densities are plotted to present the origin of the absorption peaks.

3.3.1 Design and Simulation Results

The side view of the unit cell of the proposed absorber is shown in Figure 3-6 along with wave vector, electric and magnetic field directions. The unit cell of the absorber under discussion consists of, bottom to top, the metal plate, FR4 sheet, copper wires and dielectric absorber. The copper wires are placed on the FR4 sheet, which has the permittivity and dielectric loss tangent, 4.2 and 0.02 respectively. The conductivity of copper is $5.8 \times 10^7 S/m$. The dimensions of the proposed absorber are referred as thickness of FR4 sheet (t_{fr}) =1mm, length of wire elements (l) = 5.2mm, width of wire elements (w) = 0.8mm, thickness of copper wires (t_{co}) = 0.035mm, unit cell dimension (p) = 10mm, thickness of dielectric absorber (d) = 2mm.

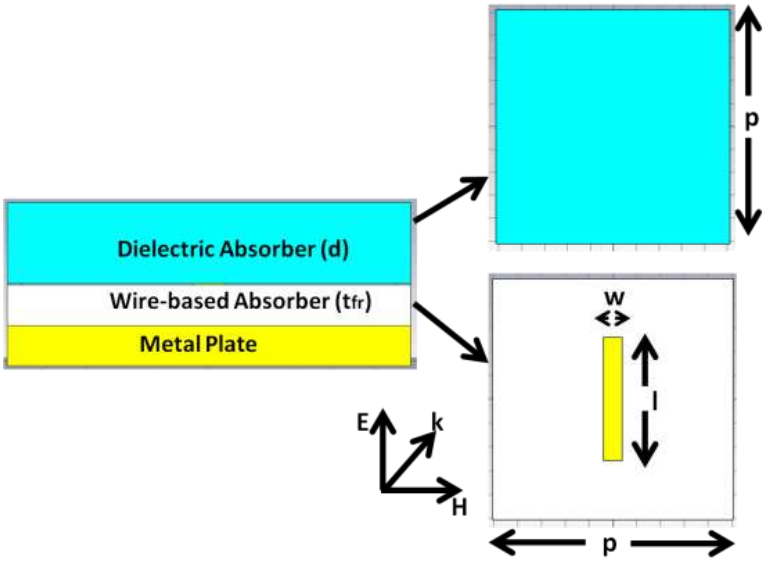

Figure 3-6: Side view of the unit cell of the proposed absorber along with wave vector, electric field and magnetic field directions

The performance of the absorber under consideration is simulated in CST Microwave Studio using frequency-domain solver with unit cell boundary conditions and directions for wave vector, electric field and magnetic field, as shown in Figure 3-6. The absorbance of the metal back absorber is calculated from the expression $A(\omega) = 1 - R(\omega) = 1 - |S_{11}|^2$. The designed absorber comprises a single wire which acts as a dipole which reduces the reflection in both cross and co-polarization. Owing to polarization sensitivity of the proposed absorber, the simulation results are presented for the field quantities orientated as shown in Figure 3-6.

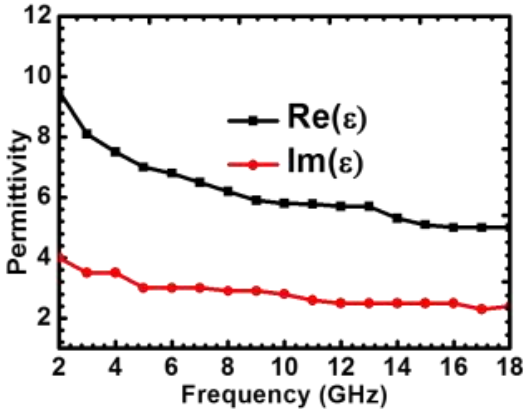

Figure 3-7: Representative and retrieved values of the real and imaginary part of permittivity (*Source:* Zhang, et al., 2014)

The designed absorber consists of the dielectric material based absorber. The EM characterization of the dielectric absorber is carried out by real and imaginary of the permittivity owing to the non-magnetic response. The arbitrary values of real and imaginary parts of permittivity cannot be considered due to Kramers-Kronig relations. Considering this, the reported values of permittivity are taken for realistic and practical design. The representative and retrieved values of real and imaginary values of permittivity [Zhang et al., 2014] are presented in Figure 3-7. The real and imaginary part of permittivity as shown in Figure 3-7 can be physically realized by adding conducting filler (carbon fibre, graphene, conducting carbon) in the polymer matrix [Qin and Brosseau, 2012]. The real and imaginary part of the permittivity, as shown in Figure 3-7, are plugged in the dispersive material list and fitted with the n^{th} order with maximum order 3. Owing to the non-magnetic response of the dielectric absorber, the real and imaginary parts of the permeability are plugged in as 1 and 0.01 respectively.

Figure 3-8(a) shows the simulated return loss for the dielectric absorber for the permittivity values shown in Figure 3-7. It is noted from that as the thickness of the dielectric absorber increases, the resonant peak shifts to a lower frequency. The behaviour dielectric absorber can be discussed using $\lambda/4$ model [Watts *et al.*, 2012]. A single resonant mode is noted for different thickness values.

Figure 3-8(b) indicates the numerical plot of the return loss of wire-based absorber for different wire element length. It is observed that as the wire element length increases, the resonant frequency shifts to the lower region, which suggests the inverse relation between the wire element length and resonant frequency [Pang *et al.*, 2013]. A single resonant mode is observed to wire element length.

The single peak is observed in dielectric and wire-based metamaterial absorber, which is attributed to material response (Z_d) and RLC resonator (Z_{FSS}) respectively. In the light of Figure 3-8, an attempt has been made to increase the bandwidth of the absorber, by overlapping the resonant mode excited by a dielectric material and metamaterial response. The simulated return loss of the proposed absorber is shown in Figure 3-9(a) for different wire element length. It is noted that for small wire length, only a single resonant peak arises, due to the dielectric absorber.

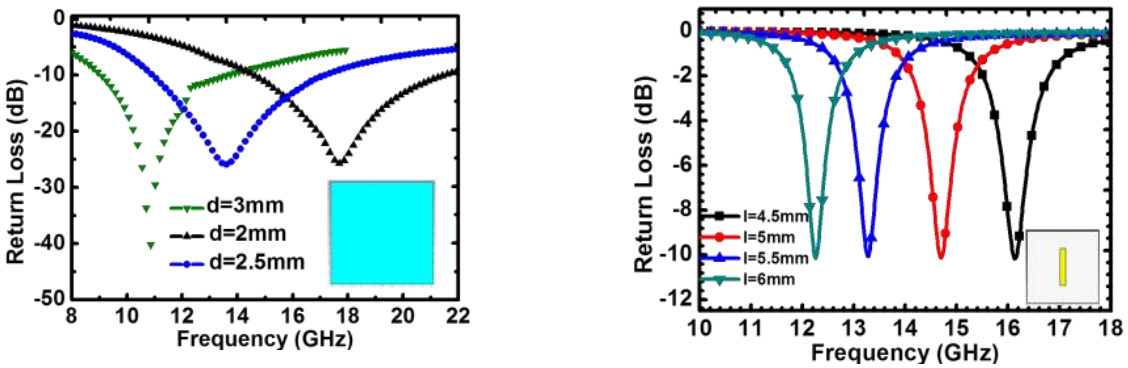

(a) (b)

Figure 3-8: (a) Simulated return loss of the dielectric absorber for different thickness (b) Simulated return loss of wire-based metamaterial absorber for different wire length and tfr = 1mm

As the wire element length increases, the second resonant mode induces due wire element length. By optimizing the design parameters viz. length of wire element and thickness of dielectric absorber, the two modes selectively overlap and result in widening the bandwidth of the absorber. For wire element length l = 5.2 mm and thickness of dielectric absorber (d) = 2mm, the two modes overlap and yields in the bandwidth of more than 6 GHz for 10 dB return loss. From Figure 3-9(a), as the dielectric material thickness is not changing the resonant mode corresponds to 10 GHz is almost invariant. Figure 3-9(b) shows the simulated absorptivity of the designed absorber for l=5.2mm and d=2mm. The absorber under discussion exhibits more than 6 GHz bandwidth, ranging from 8.4 to 15.1 GHz, for 90% absorptivity. The two peaks are observed of absorptivity 98.8 % and 98.6 % at frequencies 9.9 GHz and 12.7 GHz respectively. The reflection of the proposed absorber for cross-polarization is below -80 dB, which is almost nil (Figure 3-9(c)). The absorber response is simulated for a different angle of incidence to determine the angular stability of the absorber for practical applications, as shown in Figure 3-9(d). The performance of absorber is stable up to an angle of incidence 30°.

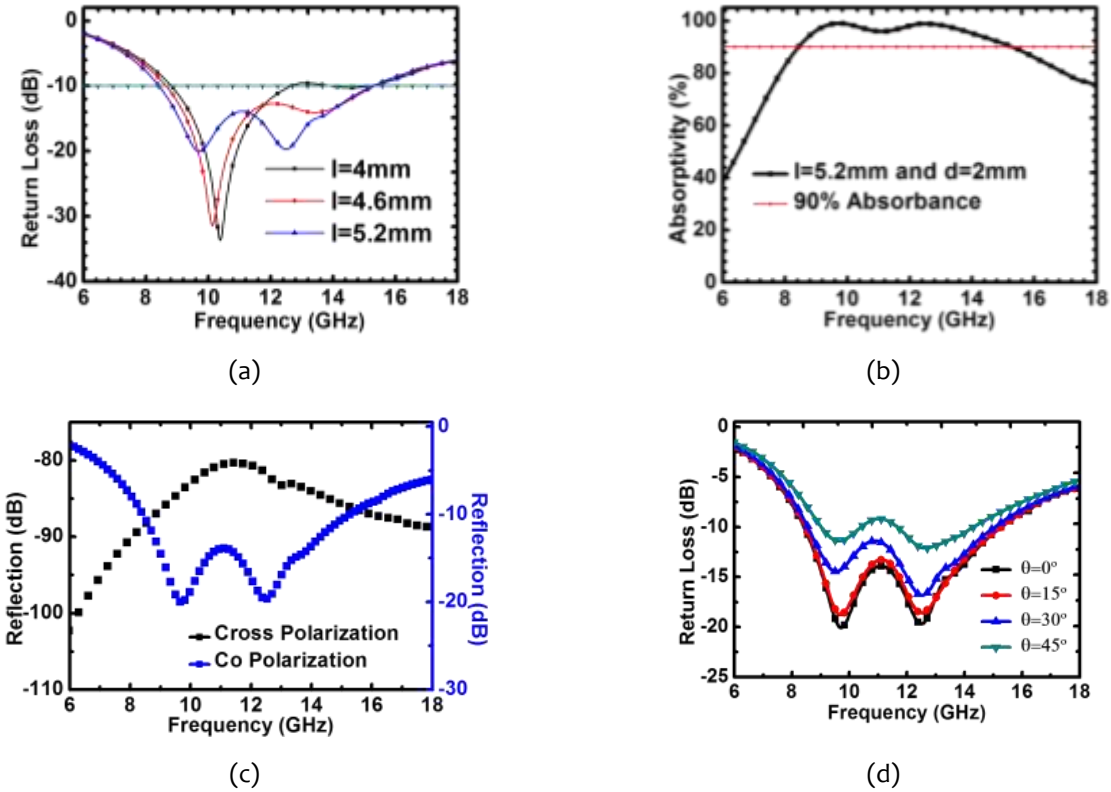

(a) (b)

(c) (d)

Figure 3-9: (a) Simulated return loss of the designed absorber for different wire element length (l), (b) Simulated absorptivity (c) Co and Cross polarization reflection of the absorber for l = 5.2mm and d = 2mm (d)

`

Simulated return loss for a different angle of incidence

3.3.2 Physical Insight

To present the physical insight and loss mechanism of the designed absorber, the electric field and power loss densities are investigated numerically at absorbing frequencies (9.7 and 12.5 GHz) for l=5.2mm, d=2mm. The electric field at 9.7 GHz is confined in the dielectric absorber due to dielectric nature whereas, at 12.5 GHz, it is at the edges of the wire elements due to dipole behaviour of the wire element. The power loss density at 9.7 GHz indicates the power loss in dielectric absorber as a dielectric loss. In contrast to this at 12.5 GHz, the power loss takes place at edges of wire elements as dielectric loss due to confinement of the electric field. The field density plots support the claim for overlapping the resonance mode induced due to dielectric material response and wire-based metamaterial response.

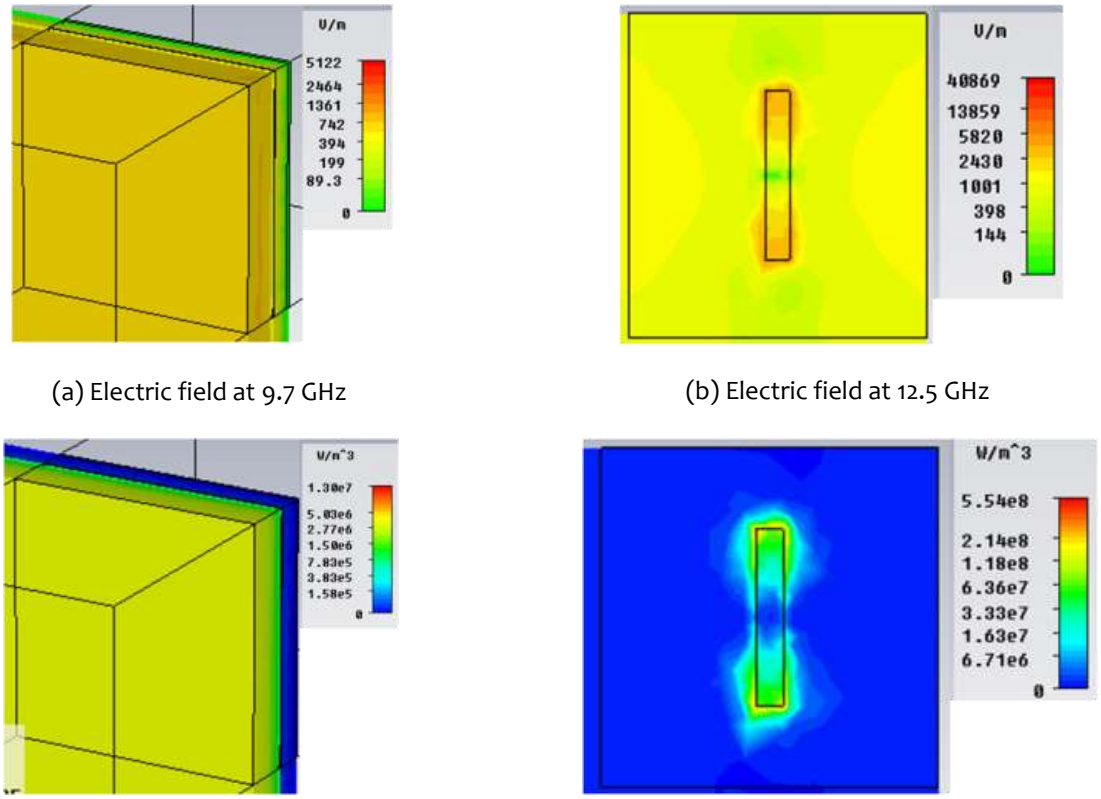

(a) Electric field at 9.7 GHz

(b) Electric field at 12.5 GHz

(c) Power loss density at 9.7 GHz

(d) Power loss density at 12.5 GHz

Figure 3-10: Electric field and power loss density at absorbing frequencies 9.7 GHz and 12.5 GHz of the proposed absorber for l=5.2mm and d=2mm

As a conclusion, two resonating modes are induced in the designed absorber using wire element and dielectric absorber as a cap layer. Bandwidth improvement is achieved by the overlapping of resonating modes excited by the dielectric absorber and wire-based metamaterials absorber. The designed absorber offers the bandwidth of more than 6 GHz for 10dB return loss. Nevertheless, due to lack of the fourfold symmetry, this design is polarization sensitive.

…